Maximum Power Point Tracking and Voltage Control in a Solar-PV based DC Microgrid Using Simulink

Frank Miyagishima¹, Sijo Augustine¹, Olga Lavrova¹, Hamed Nademi¹, Satish Ranade¹ Matthew J. Reno²,

¹ Electrical and Computer Engineering Department,
Klipsch School of Electrical and Computer Engineering
New Mexico State University, Las Cruces, NM 88003
² Sandia National Laboratories, Albuquerque, NM, 87185, USA

Abstract — This paper discusses a solar photovoltaic (PV) DC microgrid system consisting of a PV array, a battery, DC-DC converters, and a load, where all these elements are simulated in MATLAB/Simulink environment. The design and testing entail the functions of a boost converter and a bidirectional converter and how they work together to maintain stable control of the DC bus voltage and its energy management. Furthermore, the boost converter operates under Maximum Power Point Tracking (MPPT) settings to maximize the power that the PV array can output. The control algorithm can successfully maintain the output power of the PV array at its maximum point and can respond well to changes in input irradiance. This is shown in detail in the results section.

Keywords — DC microgrid, PV array, boost converter, bidirectional buck/boost converter, battery, maximum power point tracking, perturb and observe, controller, smart load management.

I. INTRODUCTION

The Department of Energy (DOE) defines the microgrid as "a group of interconnected loads and distributed energy resources within clearly defined electrical boundaries that acts as a single controllable entity with respect to the grid" [1]. One concern is the efficiency at which it can generate renewable power, deliver power to a load, and operate an energy storage system using certain methods such as maximum power point tracking (MPPT) and smart load management (SLM).

In DC microgrids, PV arrays are often employed along with DC-DC converters [2]. PV converters can operate in MPPT, wherein the goal is to track and maintain the settings at which the PV array can deliver maximum power to the grid [3], [4]. There are multiple optimization techniques employing MPPT, such as incremental conductance [5], and the most used is Perturb and Observe (P&O).

This work was partially supported by the NSF Grants \#OIA-1757207 (NM EPSCoR), HRD-1345232, HRD-1914635 and funding from the Laboratory Directed Research and Development program at Sandia National Laboratories, and funding from the Electric Utility Management Program (EUMP) at the New Mexico State University. Sandia National Laboratories is a multi-mission laboratory managed and operated by National Technology and Engineering Solutions of Sandia, LLC., a wholly owned subsidiary of Honeywell International, Inc., for the U.S. Department of Energy's National Nuclear Security Administration under contract DE-NA0003525. The views expressed in the article do not necessarily represent the views of the U.S. Department of Energy or the United States Government.

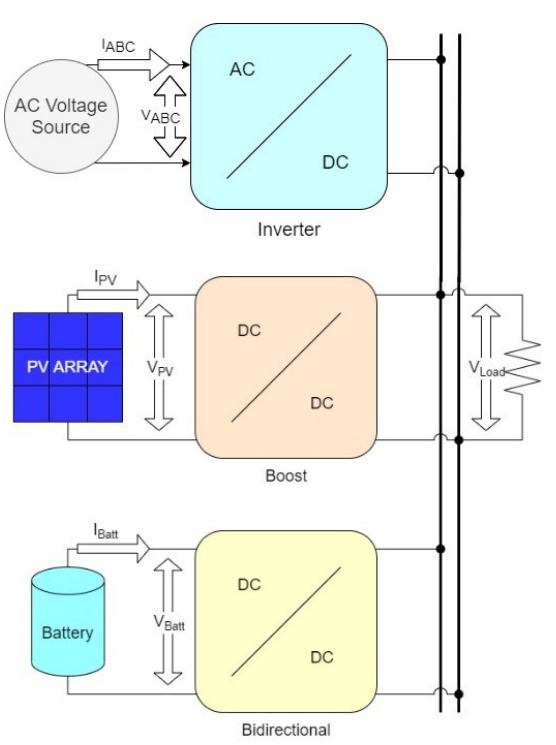


Fig. 1. Basic topology of DC microgrid used in this example.

Energy management is achieved using a battery storage system attached to a DC-DC bidirectional converter that can charge and discharge the battery. The function is to discharge the battery if the PV voltage is less than the required DC bus voltage and to charge the battery if the PV voltage is greater than the DC voltage [6].

II. SLM ARCHITECTURE

As shown in Fig. 1, the DC microgrid can be broken down into four parts for further analysis: The PV array, the DC bus, the energy storage, and the AC grid voltage. Each of these components and the interactions between them are explained further in the following sections.

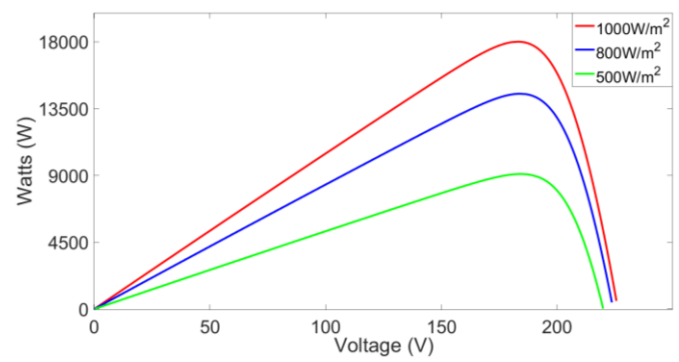


Fig. 2. P-V curves of the PV array at three different irradiance values.

The PV array is the main source of power in the microgrid. It is connected to a boost converter operating under MPPT control to provide the PV array with the optimal conditions for power generation by directly controlling the duty ratio of the converter.

The battery is a Nickel-Metal-Hydride battery rated with a nominal voltage of 300V. It is connected to a buck/boost bidirectional converter controlled using PID controllers to regulate the voltage of the DC bus. The capacity of the battery is changed to different ratings to show how the State of Charge (SoC) is affected. For the first simulation of a grid-connected system, the battery is rated for a capacity of 50Ah.

The AC grid voltage is a voltage source connected in parallel to the DC bus used to simulate a connection to the main grid. The voltage operates at $480V_{RMS}$ and is connected through an LC filter and an inverter operating at 4000Hz.

III. SYSTEM DESIGN

The parameters (capacitance, inductance, source voltage, etc.) were selected with the purpose of optimizing the performance of the microgrid and its components. The configuration of this microgrid is based on the requirement that the DC bus must operate at a controlled voltage of 380V. To test the efficiency of this controller and the battery cycles, the irradiance of the PV array is changed between three different values as shown in Fig. 2, with each irradiance value producing a different MPP. The parameters are summarized in Table I.

The converters used are a boost converter connected in series with the PV array, a buck/boost bidirectional converter in series with the battery, and an AC/DC inverter in series with the AC voltage. Both capacitors for the bidirectional converter have a capacitance of 1mF while the output capacitor for the boost converter has a capacitance of $100\mu F$.

IV. CONTROLLER CONFIGURATIONS

The boost converter uses an MPPT setting to control the duty ratio of the gate voltage. The MPPT controller operates on a P&O method using a MATLAB function block. The block takes the PV array voltage and current as inputs and outputs the duty ratio to a PWM (pulse width modulation) generator. The implementation of this algorithm can be explained in Fig. 3 [8].

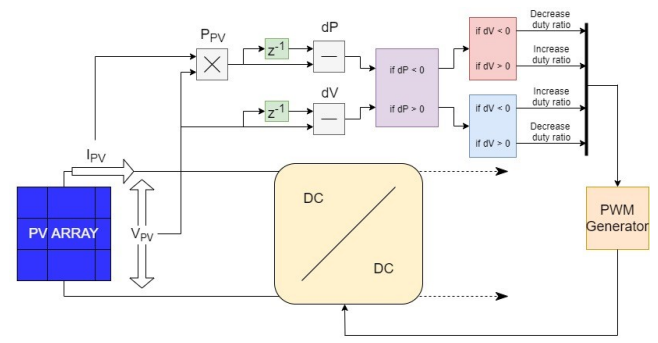


Fig. 3. Control diagram of MPPT for boost converter.

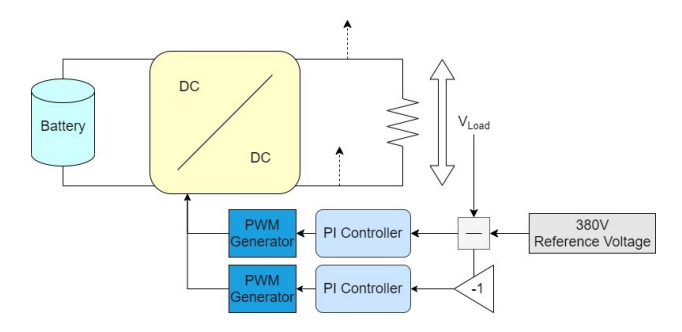


Fig. 4. Control diagram of voltage control for bidirectional converter.

This algorithm measures the voltage and current in the PV bus, calculates the power, and compares these values to their previous iteration then it will either increase or decrease the duty ratio as needed. In the next time sample step, the code runs again using the next measurements of voltage and current. This MATLAB code is executed every 1µs and has a duty ratio perturbation of 5E-6.

The DC-DC bidirectional converter is controlled by a pair of PI controllers using the voltage reference set at 380V. The controller takes the voltage measurement from the DC bus and compares it to the reference voltage to regulate the DC voltage using the battery cycles [9]. The two PI controllers have the same configuration but each controls one MOSFET of the buck/boost converter. When the battery needs to be charged the controller pair shuts off the boost converter and controls the buck converter, likewise when the battery needs to be discharged the buck converter is shut off and the boost converter is controlled. This configuration is taken from the setup used in [10] and adjusted to fit into this model. The process is depicted in Fig. 4.

The inverter uses a conventional 6-pulse PWM generator to control the inverter IGBTs. The generator operates under uses a carrier frequency of 4000Hz and a reference frequency of 60Hz.

V. ANALYSIS & RESULTS

The simulation starts with an input irradiance of 1000W/m^2 for t = [0,10] seconds. The PV array power measurement clears its first transient state within 90ms and settles at 17.992kW (effectively 99.91% of the theoretical MPP 18.007kW according to Fig. 2) with a ripple of 54W peak-to-peak. The voltage clears its transient state in 1.5s and stabilizes at 380.5V

with a ripple of 4V peak-to-peak. At t = 10s, the battery SoC peaks at 30.07% as the surplus power is used to charge the battery.

When irradiance drops to 500W/m^2 at t=10 s the power enters its second transient state for 200ms then settles at 9.050 kW (99.49% of the current MPP 9.096 kW) with a ripple of 220W peak-to-peak. The voltage settles after 240ms at 380.5 V with a ripple of 28.5 V peak-to-peak. At t=15 s the battery has discharged back to 30% as the DC bus voltage measures short of the voltage reference.

At t=15s irradiance rises to $800W/m^2$. Power settles at 14.481kW (99.85% of 14.502kW) after 60ms with a ripple of 57W peak-to-peak. Voltage settles at 380.44V after 600ms with a ripple of 4.4V peak-to-peak. The SoC at t=25s decreases to 29.995%. The smaller discharge is due to the DC bus voltage being closer to the reference than with the previous irradiance.

The measurements of power, voltage, and SoC against time are shown in Fig. 5, Fig. 6, and Fig. 7, respectively. Fig. 8 shows the SoC against time for different battery capacity ratings while also operating the microgrid in "islanded mode" for simplicity. This is to show how a different capacity can affect the charging and discharging rates without changing how much power is being delivered or generated by the battery. Table II lists the differences in rates and the SoC between the different batteries. These ramp rates from the power electronics can be important in the design of the protection system and relay settings in DC microgrids [11-14].

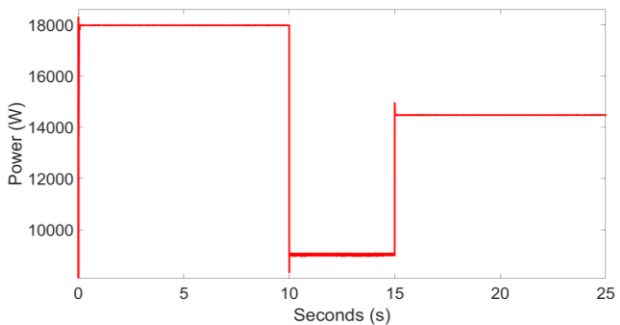


Fig 5. PV power measurements against time.

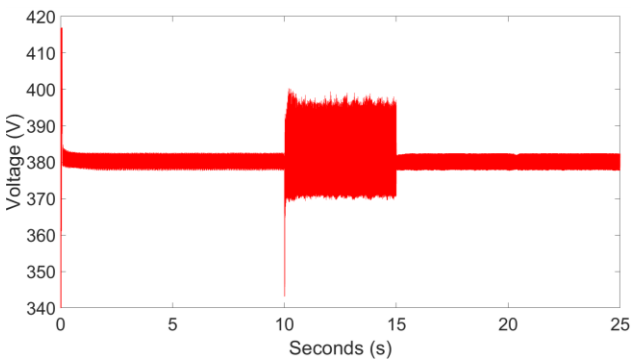


Fig. 6. DC voltage measurements against time.

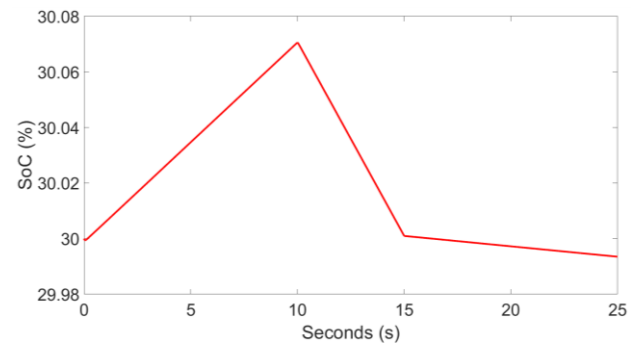


Fig. 7. State of Charge against time.

TABLE I System Parameters

Parameter	Value	Unit
Converter inductances	1	mН
Boost converter capacitance	100	μF
Bidirectional converter capacitances	1	mF
DC bus load resistance	10	Ω
PV array V _{OC}	226.2	V
PV array I _{SC}	106.2	A
PV array V _{MP}	183	V
PV array I _{MP}	98.4	A
Battery nominal voltage	300	V
Battery capacity	50	Ah
Battery initial SoC	30	%
Nominal switching frequency	20	kH
AC Voltage Source	480	V_{RMS}
LC filter inductance	10	mН
LC filter capacitance	1	uF

TABLE II BATTERY MEASUREMENTS

Time	5Ah		10Ah		50Ah	
	Rate	End	Rate	End	Rate	End
	(s)	SoC	(s)	SoC	(s)	SoC
		(%)		(%)		(%)
0-10s	0.045	29.97	0.022	30.23	0.004	30.04
10–15s	-0.108	29.43	-0.048	29.99	-0.009	30.00
15–25s	-0.005	29.38	-0.003	29.96	-0.001	29.99

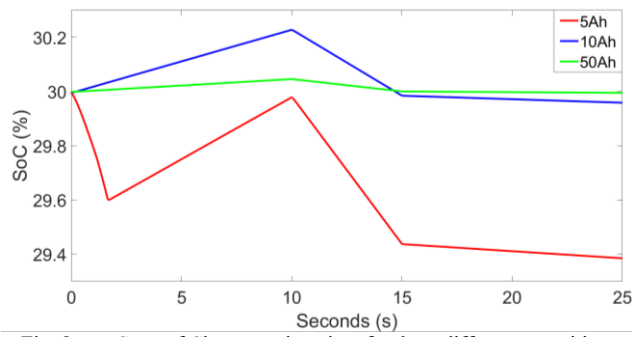


Fig. 8. State of Charge against time for three different capacities.

VI. CONCLUSIONS

The goal of this simulation is to design a DC microgrid controller that maintains the PV array's power output at the maximum point and uses a DC bus reference voltage to regulate the load voltage of the microgrid. The purpose is also to showcase the differences in battery cycles with varying Ah capacities. The model produces satisfying results given these select requirements.

- [1] Ton, Dan & Smith, Merrill. (2012). The U.S. Department of Energy's Microgrid Initiative. The Electricity Journal. 25. 84–94. 10.1016/j.tej.2012.09.013.
- [2] D. Kumar, F. Zare, and A. Ghosh, "DC Microgrid Technology: System Architectures, AC Grid Interfaces, Grounding Schemes, Power Quality, Communication Networks, Applications, and Standardizations Aspects," in IEEE Access, vol. 5, pp. 12230-12256, 2017, doi: 10.1109/ACCESS.2017.2705914.
- [3] S. Augustine, N. Lakshminarasamma, M. K. Mishra and T. Sreekanth, "MPP tracking of PV based low voltage DC microgrid system with adaptive droop algorithm," 2015 IEEE 42nd Photovoltaic Specialist Conference (PVSC), 2015, pp. 1-4, doi: 10.1109/PVSC.2015.7356297.

- [4] A. Nigam and A. Kumar Gupta, "Performance and simulation between conventional and improved perturb & observe MPPT algorithm for solar PVcell using MATLAB/Simulink," 2016 International Conference on Control, Computing, Communication and Materials (ICCCCM), 2016, pp. 1-4, doi: 10.1109/ICCCCM.2016.7918220.
- [5] T. M. Chung, H. Daniyal, M. H. Sulaiman and M. S. Bakar, "Comparative study of P&O and modified incremental conductance algorithm in solar maximum power point tracking," 4th IET Clean Energy and Technology Conference (CEAT 2016), 2016, pp. 1-6, doi: 10.1049/cp.2016.1300.
- [6] Shatakshi, B. Singh and S. Mishra, "Dual mode operational control of single stage PV-battery based microgrid," 2018 IEEMA Engineer Infinite Conference (eTechNxT), 2018, pp. 1-5, doi: 10.1109/ETECHNXT.2018.8385379.
- [7] B. Hauke, "Basic Calculation of a Boost Converter's Power Stage," Application Report, Texas Instruments, SLVA372C, January 2014.
- [8] S. N. Patil and R. C. Prasad, "Design and development of MPPT algorithm for high efficient DC-DC converter for wind energy system connected to grid," 2015 International Conference on Computer, Communication and Control (IC4), 2015, pp. 1-7, doi: 10.1109/IC4.2015.7375634.
- [9] S. Jadhav, N. Devdas, S. Nisar and V. Bajpai, "Bidirectional DC-DC converter in Solar PV System for Battery Charging Application," 2018 International Conference on Smart City and Emerging Technology (ICSCET), 2018, pp. 1-4, doi: 10.1109/ICSCET.2018.8537391.
- [10] Ortiz, Leony, et al. "Hybrid AC/DC Microgrid Test System Simulation: Grid-Connected Mode." Heliyon, vol. 5, no. 12, Elsevier BV, Dec. 2019, p. e02862, doi:10.1016/j.heliyon.2019.e02862.
- [11] R. Montoya, B. Poudel, A. Bidram, M. J. Reno, "DC Microgrid Fault Detection Using Multiresolution Analysis of Traveling Waves," International Journal of Electric Power & Energy Systems, 2022.
- [12] S. Augustine, M. J. Reno, S. M. Brahma, and O. Lavrova, "Fault Detection and Current Control for a Standalone DC Microgrid Using Current Derivative and Adaptive Droop," Journal of Emerging and Selected Topics in Power Electronics, 2020.
- [13] S. Augustine, J. E. Quiroz, M. J. Reno, and S. Brahma, "DC Microgrid Protection: Review and Challenges," Sandia National Laboratories, SAND2018-8853, 2018.
- [14] S. Paruthiyil, R. Montoya, A. Bidram, and M. J. Reno, "A Numerical Method for Fault Location in DC Systems Using Traveling Waves," IEEE North American Power Symposium (NAPS), 2021.